Neuron
Report

Functional Significance of Isoform Diversification in the Protocadherin Gamma Gene Cluster

Weisheng V. Chen,[1] Francisco J. Alvarez,[2,5] Julie L. Lefebvre,[3] Brad Friedman,[1,6] Chiamaka Nwakeze,[1] Eric Geiman,[2] Courtney Smith,[2] Chan Aye Thu,[1] Juan Carlos Tapia,[1] Bosiljka Tasic,[4] Joshua R. Sanes,[3] and Tom Maniatis[1,*]
[1]Department of Biochemistry and Molecular Biophysics, Columbia University Medical Center, 701 W. 168 Street, New York, NY 10032, USA
[2]Department of Neuroscience, Physiology and Cell Biology, Wright State University School of Medicine, 3640 Colonel Glenn Highway, Dayton, OH 45435, USA
[3]Center for Brain Science and Department of Molecular and Cellular Biology, Harvard University, 52 Oxford Street, Cambridge, MA 02138, USA
[4]Allen Institute for Brain Science, 551 N. 34 Street, Seattle, WA 98103, USA
[5]Present address: Department of Physiology, Emory University School of Medicine, 615 Michael Street, Atlanta, GA 30322, USA
[6]Present address: Department of Bioinformatics and Computational Biology, Genentech, Inc., 1 DNA Way, South San Francisco, CA 94080, USA
*Correspondence: tm2472@columbia.edu
http://dx.doi.org/10.1016/j.neuron.2012.06.039

SUMMARY

The mammalian Protocadherin (*Pcdh*) alpha, beta, and gamma gene clusters encode a large family of cadherin-like transmembrane proteins that are differentially expressed in individual neurons. The 22 isoforms of the *Pcdhg* gene cluster are diversified into A-, B-, and C-types, and the C-type isoforms differ from all other clustered Pcdhs in sequence and expression. Here, we show that mice lacking the three C-type isoforms are phenotypically indistinguishable from the *Pcdhg* null mutants, displaying virtually identical cellular and synaptic alterations resulting from neuronal apoptosis. By contrast, mice lacking three A-type isoforms exhibit no detectable phenotypes. Remarkably, however, genetically blocking apoptosis rescues the neonatal lethality of the C-type isoform knockouts, but not that of the *Pcdhg* null mutants. We conclude that the role of the *Pcdhg* gene cluster in neuronal survival is primarily, if not specifically, mediated by its C-type isoforms, whereas a separate role essential for postnatal development, likely in neuronal wiring, requires isoform diversity.

INTRODUCTION

Protocadherins (Pcdhs) are the largest subgroup of the cadherin superfamily of cell adhesion proteins. Of the ~70 *Pcdh* genes identified in mammalian genomes, over 50 are located in three tightly linked gene clusters (*Pcdha*, *Pcdhb*, and *Pcdhg*) on a single chromosome (Wu and Maniatis, 1999). These clustered *Pcdh* genes are found exclusively in vertebrates and are predominantly expressed in the nervous system. Distinct subsets of *Pcdh* genes are differentially expressed in individual neurons, and enormous cell surface diversity may result from combinatorial expression (Esumi et al., 2005; Kaneko et al., 2006; Kohmura et al., 1998; Wang et al., 2002a). A subset of Pcdhg isoforms have been shown to engage in intercellular interactions that are strictly homophilic (Schreiner and Weiner, 2010). The molecular diversity as well as the binding specificity of clustered Pcdhs has led to the proposal that they provide a synaptic address code for neuronal connectivity or a single-cell barcode for self-recognition and self-avoidance similar to that ascribed to Dscam1 proteins of invertebrates (Junghans et al., 2005; Serafini, 1999; Shapiro and Colman, 1999; Zipursky and Sanes, 2010).

Genetic manipulations of individual *Pcdh* gene clusters in mice have provided functional evidence that the clustered Pcdhs are required for normal development of the nervous system. Mutations in the *Pcdha* gene cluster have been reported to result in defects in olfactory sensory neuron axon coalescence and serotonergic axonal arborization as well as behavioral perturbations (Fukuda et al., 2008; Hasegawa et al., 2008; Katori et al., 2009). By contrast, abolishing Pcdhg function leads to neuronal apoptosis and synaptic loss in the spinal cord and retina (Lefebvre et al., 2008; Prasad et al., 2008; Wang et al., 2002b; Weiner et al., 2005). Although these genetic studies have provided interesting insights into the roles of clustered Pcdhs in the nervous system, the functional significance of the diverse isoforms encoded by the three gene clusters is not understood. For example, it is unclear whether individual Pcdh isoforms within each cluster are functionally equivalent or whether certain isoforms may play distinct roles. The unique and highly conserved genomic organization of *Pcdh* gene clusters suggests that the isoform diversity and evolutionary diversification of *Pcdh* genes are central to understanding their function.

In mice, the three *Pcdh* gene clusters each contain 14-22 homologous "variable" exons arrayed in tandem. Each variable exon is transcribed from its own promoter, and encodes the entire extracellular domain, a transmembrane domain, and a short intracellular domain of the corresponding Pcdh protein. In *Pcdha* and *Pcdhg* clusters (but not *Pcdhb* cluster), these variable exons are followed by a set of three "constant" exons, which are joined to each variable exon via *cis*-splicing to encode

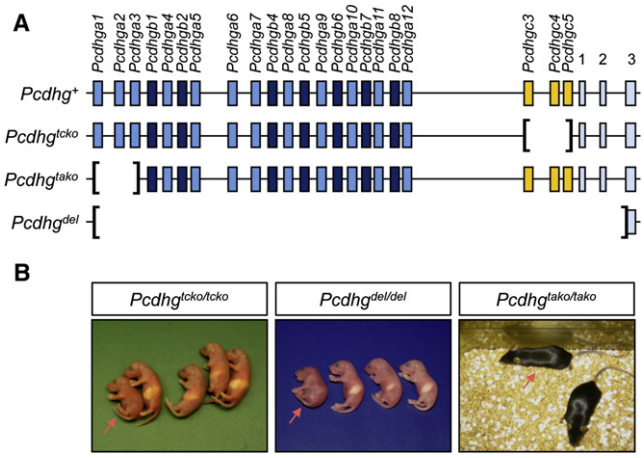

Figure 1. *Pcdhg* Mutant Alleles and Phenotypes

(A) Schematic representations of *Pcdhg* wild-type and mutant alleles. (B) Gross phenotypes of $Pcdhg^{tcko/tcko}$ (P0), $Pcdhg^{del/del}$ (P0), and $Pcdhg^{tako/tako}$ (P60) mutants as compared to littermate controls. Homozygous mutants are indicated with a red arrow. See also Figure S1 and Movie S1.

a common distal intracellular domain (Tasic et al., 2002; Wang et al., 2002a). An interesting feature of the genomic organization of the *Pcdh* gene clusters is that the last two variable exons in the *Pcdha* cluster, as well as the last three variable exons in the *Pcdhg* cluster, are more similar to each other than to other variable exons within their respective cluster (Wu et al., 2001). These 5 *Pcdh* genes (*Pcdhac1*, *Pcdhac2*, *Pcdhgc3*, *Pcdhgc4*, and *Pcdhgc5*) are designated C-type genes, to be distinguished from A-type and B-type genes of the *Pcdhg* cluster. The C-type isoforms bear several unique features among all Pcdhs: (1) while all other Pcdhs are more closely related to members within their own cluster, C-type isoforms are evolutionarily divergent, forming a separate branch in the phylogenetic tree (Wu and Maniatis, 1999; Wu et al., 2001); (2) three out of the five C-type genes (*Pcdhac2*, *Pcdhgc4*, and *Pcdhgc5*) lack the conserved sequence element (CSE) found in the promoters of all other *Pcdh* genes (except *Pcdhb1*), suggesting that these genes are regulated differently (Wu et al., 2001); (3) single-cell RT-PCR experiments indicated that, while other *Pcdh* genes are stochastically and monoallelically expressed in Purkinje neurons, every neuron expresses all five C-type genes from both chromosomes (Esumi et al., 2005; Kaneko et al., 2006). Taken together, these observations suggest that the C-type isoforms play unique and essential roles among all clustered Pcdhs. To investigate this possibility, we generated mutant mice lacking the three C-type genes (*Pcdhgc3*, *Pcdhgc4*, *Pcdhgc5*) in the *Pcdhg* cluster.

RESULTS

Mice Lacking the C-Type *Pcdhg* Genes Are Phenotypically Indistinguishable from Mice Lacking the Entire *Pcdhg* Cluster

The triple C-type isoform knockout (TCKO) allele was generated by deleting the three variable exons (Figure 1A and see Figures S1A and S1C available online), which specifically removes the C-type genes without affecting the splicing of the remaining 19 A-type and B-type *Pcdhg* variable exons (see below). $Pcdhg^{tcko/tcko}$ mutants are born alive at the normal Mendelian ratio but invariably die during the first day after birth. The mutant mice are readily distinguishable from wild-type and heterozygous littermates by a characteristic hunched posture and limb tremors, as well as by severely compromised voluntary movements and reflexes (Figure 1B and Movie S1). Remarkably, these phenotypes are identical to those described for the *Pcdhg* full cluster deletion mice (Figure 1B and Movie S1), in which all *Pcdhg* isoforms are abolished (Wang et al., 2002b). In addition to the common phenotypes described above, we found that both lines of mutants also exhibit intense muscle stiffness and umbilical hernia (Figure S1D). Interestingly, these phenotypes closely resemble those of mutant mice deficient in VGAT (Wojcik et al., 2006), GAD67 (Asada et al., 1997), and Gephyrin (Feng et al., 1998), which are essential components for GABA and glycine production and transmission.

While the virtually identical phenotypes of the $Pcdhg^{tcko/tcko}$ and $Pcdhg^{del/del}$ mutants demonstrate that C-type isoforms are essential, it is also possible that the entire repertoire of *Pcdhg* genes are required; that is, each isoform is indispensable. Indeed, essentially every *Pcdhg* gene in humans has an ortholog in the mouse, in contrast to the *Pcdha* and *Pcdhb* genes (Wu et al., 2001). To address this possibility, we deleted *Pcdhga1*, *Pcdhga2*, and *Pcdhga3* genes in the mouse (Figures 1A, S1B, and S1C). The triple A-type isoform knockout (TAKO) mutants are viable and fertile, and survive to adulthood with no discernible abnormalities (Figure 1B and Movie S1).

$Pcdhg^{tcko/tcko}$ and $Pcdhg^{del/del}$ Mutants Display Similar Levels and Patterns of Neuronal Cell Loss in the Spinal Cord

Previous studies showed that deletion of the *Pcdhg* cluster leads to extensive apoptosis and eventual loss of specific subpopulations of spinal interneurons (Prasad et al., 2008; Wang et al., 2002b; Weiner et al., 2005). To determine whether these changes also occur in TCKO mutants, we labeled cells undergoing apoptosis with anti-cleaved caspase-3 in P0 spinal cords. As expected, the number of apoptotic profiles is markedly increased in the spinal cord of both $Pcdhg^{tcko/tcko}$ and $Pcdhg^{del/del}$ mutants (Figures 2A–2A″). Concurrently, the spinal cords of both mutants exhibit similar levels of astrogliosis and microglia activation (Figures S2A), which typically accompany neuronal cell death. To compare the extent of neuronal cell loss in different *Pcdhg* mutant lines, we quantified the surviving $NeuN^+$ neurons in different spinal regions at P0. The spinal cords of $Pcdhg^{tcko/tcko}$ and $Pcdhg^{del/del}$ mutants have a similarly reduced cross-sectional area compared to those of the wild-type littermates, particularly in the ventral horn (LVI-VIII) and in the deep dorsal horn (LIV-V). Superficial dorsal horn (LI-III) and motor pools (LIX), however, appear relatively normal (Figures 2B–2B″ and S2B). Consistently, the most severe neuronal loss was detected in the ventral horn and to a lesser extent in the deep dorsal horn (~70% and ~50%, respectively). We also observed ~30% interneuron cell loss in the superficial dorsal horn, which was not reported previously. By contrast, motor neuron (LIX) counts in both mutants are the same as

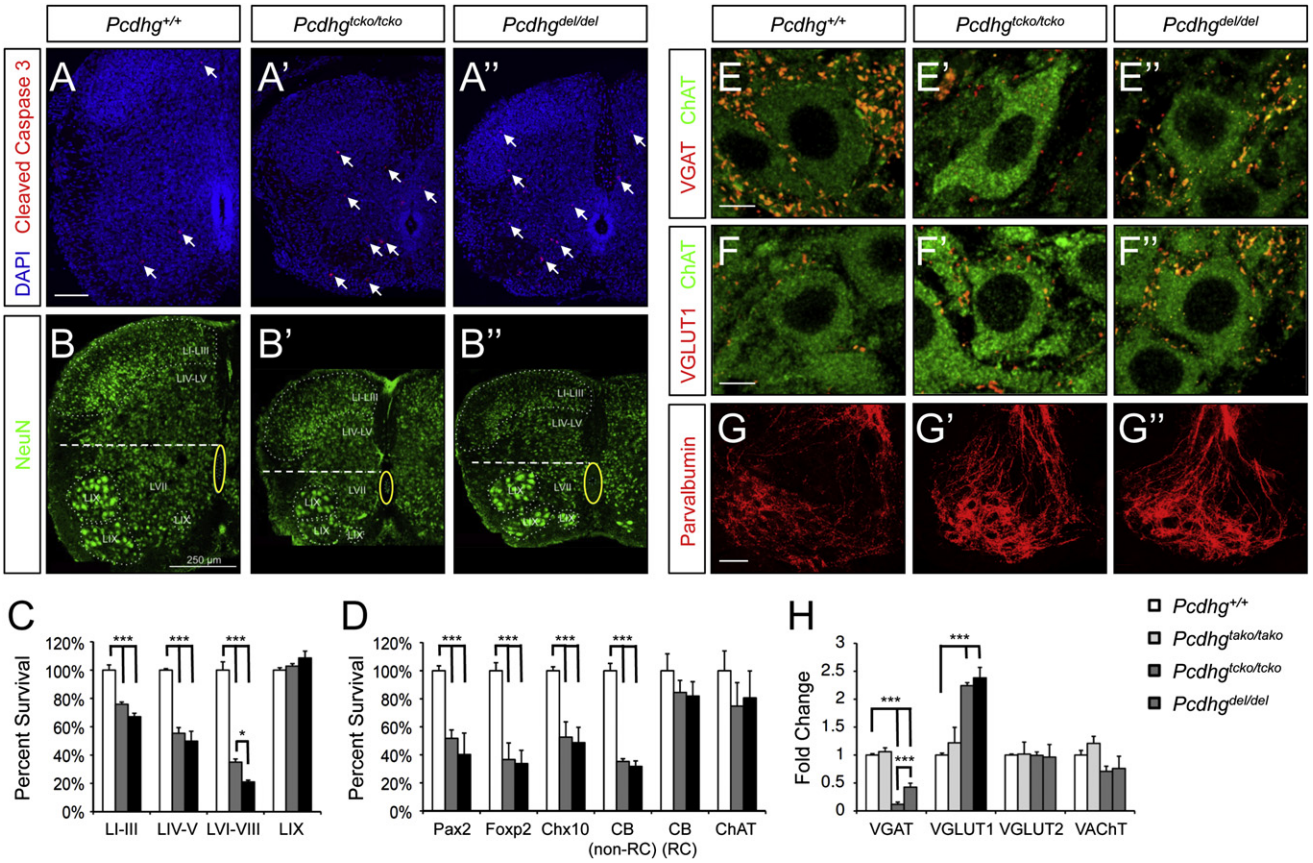

Figure 2. Similar Levels and Patterns of Neuronal Loss and Synaptic Changes in the Spinal Cord of *Pcdhg*$^{tcko/tcko}$ and *Pcdhg*$^{del/del}$ Mutants

(A–A″) Both mutants exhibit increased levels of apoptosis as indicated by the increased numbers of cleaved caspase 3$^+$ profiles (arrows). Scale bar: 100 μm. (B–B″) Quantitative analyses of surviving neuronal populations in different lamina. NeuN$^+$ neurons of distinct laminar regions are indicated. The central canal area is highlighted with a yellow oval, and the spinal cord is horizontally bisected with a dashed line to indicate the dorsal horn and the ventral horn areas. Scale bar: 250 μm. (C) Percent survival of NeuN$^+$ neuronal populations according to their laminar locations (LI-LIX) in homozygous mutants, calculated by normalizing neuronal counts to wild-type controls. Error bars represent SEM. *$p < 0.05$, ***$p < 0.001$. Details of the quantitative analyses can be found in Figure S2B. (I) Percent survival of interneuron subpopulations in the ventral horn. Representative images of Pax2, Foxp2, Chx10, CB and Chat immunolabled wild type and mutant spinal cords (P0) are shown in Figure S2C. Error bars represent SEM. ***$p < 0.001$. (E and F) VGAT$^+$ and VGLUT1$^+$ synaptic inputs onto motor neurons of wild-type and mutant spinal cords at P0. Motor neurons are labeled with anti-ChAT in green, and synaptic inputs with antibodies against different vesicular transporters in red. Scale bars: 5 μm. (G–G″) Terminal arborization of Parvalbumin$^+$ Ia primary afferents surrounding motor pools is altered in both lines of mutants. Scale bar: 50 μm. (H) Fold changes in synaptic density for each type of synapse in the mutants as calculated by normalizing to wild-type controls. Error bars represent SEM. ***$p <$ 0.001. Details of the quantitative analyses can be found in Figure S2D.

those in wild-type controls (Figures 2C and S2B). As expected, *Pcdhg*$^{tako/tako}$ spinal cords are indistinguishable from the wild-type controls, and neuronal cell counts in each of the 4 specified regions are normal (Figure S2B).

To investigate whether neuronal subpopulations are similarly affected in *Pcdhg*$^{tcko/tcko}$ and *Pcdhg*$^{del/del}$ mutants, we examined several classes of interneurons in the ventral spinal cord at P0. Interestingly, while Pax2$^+$ and Foxp2$^+$ inhibitory interneurons, as well as Chx10$^+$ excitatory interneurons are similarly reduced in number in both mutants, V1-derived Calbindin (CB)$^+$ Renshaw cells and V0-derived cholinergic ChAT$^+$ partition cells are spared (Figures 2D and S2C). In conclusion, the *Pcdhg*$^{tcko/tcko}$ and *Pcdhg*$^{del/del}$ mutants display similar levels and patterns of neuronal cell loss in the spinal cord, and interneuron subpopulations are differentially affected in both mutants.

Pcdhg$^{tcko/tcko}$ and *Pcdhg*$^{del/del}$ Mutants Display Similar Alterations in Specific Synaptic Inputs onto Motor Neurons

In addition to neuronal cell loss, a general reduction in the numbers of both excitatory and inhibitory synapses was observed in the neuropil of *Pcdhg*$^{del/del}$ spinal cords using generic synaptic markers (Wang et al., 2002b; Weiner et al., 2005). It was unclear, however, whether all synapses are similarly affected, or if certain types are spared or even increased in number. To distinguish between these possibilities, we examined major classes of synaptic inputs onto motor neurons, a cell type that receives defined synaptic inputs and survives in both *Pcdhg*$^{tcko/tcko}$ and *Pcdhg*$^{del/del}$ mutants. Four type-specific presynaptic markers were used, which respectively label synaptic vesicular transporters for the neurotransmitters

GABA and glycine (VGAT), glutamate (VGLUT1 and VGLUT2), and acetylcholine (VAChT). We found that the average linear density of VGAT$^+$ contacts was markedly decreased in both *Pcdhg*$^{tcko/tcko}$ and *Pcdhg*$^{del/del}$ mutants (Figures 2E–2E″ and 2H), whereas the number of VGLUT1$^+$ proprioceptive primary afferent inputs was surprisingly increased, more than double the number in wild-type controls (Figures 2F–2F″ and 2H). By contrast, the densities of VGLUT2$^+$ and VAChT$^+$ contacts on motor neurons remain constant (Figure 2H). As expected, all four types of synapses are unaltered in *Pcdhg*$^{tako/tako}$ mutants (Figures 2H and S2D).

The significant decrease in VGAT$^+$ synapses on motor neurons in both *Pcdhg*$^{tcko/tcko}$ and *Pcdhg*$^{del/del}$ mutants is consistent with our observation that the two mutants display identical motor defects, which closely resemble those found in the VGAT (Wojcik et al., 2006), GAD67 (Asada et al., 1997), and Gephyrin (Feng et al., 1998) knockouts. Key features of the common phenotypes are muscle stiffness and immobility, which can be explained by tetanic motor neuron activation due to compromised inhibitory neurotransmission. The reduced density of VGAT$^+$ contacts, as well as the normal numbers of VAChT$^+$ synapses in *Pcdhg*$^{tcko/tcko}$ and *Pcdhg*$^{del/del}$ mutants correlate well with the significant reduction of inhibitory interneurons and unaltered numbers of cholinergic partition cells in both mutants. By contrast, VGLUT2$^+$ synaptic density is normal despite the reduction of certain premotor glutamatergic interneurons (e.g., Chx10$^+$ V2a interneurons), which suggests that alternative neuronal sources or compensatory mechanisms might be involved in the development of these synapses.

The increased densities of VGLUT1$^+$ contacts in both *Pcdhg*$^{tcko/tcko}$ and *Pcdhg*$^{del/del}$ mutants indicate alterations in the stretch reflex circuit, where proprioceptive sensory afferents (Ia primary afferents, IaPA) establish monosynaptic contacts with spinal motor neurons innervating the same muscle (Chen et al., 2003). Centrally projecting IaPA axons (Parvalbumin$^+$) in wild-type spinal cords are distributed in an orderly fashion around motor pools, but in both mutants they appear clumped and more densely surround motor neurons, consistent with the observed increase in the density of VGLUT1$^+$ contacts (Figures 2G–2G″). The percentage of Parvalbumin$^+$ neurons in mutant dorsal root ganglia (DRG) is similar to those of wild-type animals (L2 DRG, 23.5% ± 1.3% in *Pcdhg*$^{del/del}$ and 21.8% ± 1.7% in *Pcdhg*$^{+/+}$, $p > 0.05$), indicating that the increased density of the central projections of IaPAs is not due to increased numbers of proprioceptive neurons, but rather to a defect in their terminal arborization resulting from the loss of interneurons they interact with (Jankowska, 1992). Taken together, these observations indicate that similar alterations in specific types of synapses on motor neurons occur in both *Pcdhg*$^{tcko/tcko}$ and *Pcdhg*$^{del/del}$ mutants.

Conditionally Inactivating the C-Type *Pcdhg* Genes in the Retina Recapitulates the *Pcdhg* Null Phenotype

We next extended the genetic analysis to the retina. We have shown previously that *Pcdhg* genes are required for the survival of many neuronal subpopulations in the developing inner retina but appear to be dispensable for synapse formation and function (Lefebvre et al., 2008). To generate retina-specific knockouts of TCKO and TAKO mutants, *trans*-heterozygous animals containing one conditional *Pcdhg*^{fcon3} allele (Lefebvre et al., 2008; Prasad et al., 2008) and one *Pcdhg*^{tcko} or *Pcdhg*^{tako} allele were produced. Upon retina-specific recombination of *Pcdhg*^{fcon3} that leads to a functionally null allele, the remaining *Pcdhg* isoforms are only expressed from the *Pcdhg*^{tcko} or *Pcdhg*^{tako} allele, providing a convenient way to conditionally inactivate the three C-type or A-type isoforms in postnatal animals.

We first examined the retinal architecture in conditional *trans*-heterozygous and Pcdhg null mutant animals. Retina lamination was normal and the ONL and OPL layers were unaffected in all three types of mutants. However, while the INL and IPL layers in *Pcdhg*$^{fcon3/tako}$ mutant retinas were indistinguishable from those in control, they were significantly thinner in both *Pcdhg*$^{fcon3//tcko}$ and *Pcdhg*$^{fcon3/fcon3}$ mutant retinas (Figures 3A–3A″ and 3D). Quantification of retina interneurons using cell-type-specific markers revealed that INL thinning in *Pcdhg*$^{fcon3//tcko}$ mutants is due to reduced numbers of bipolar (Chx10$^+$) and amacrine (Pax6$^+$) interneurons (Figures 3B–3B″ and 3E) as in the null (Lefebvre et al., 2008). Likewise, the loss of RGC projection neurons (Brn3a$^+$) in *Pcdhg*$^{fcon3/tcko}$ *trans*-heterozygous retinas is equal in severity to that of *Pcdhg*$^{fcon3/fcon3}$ mutants (Figures 3C–3C″ and 3E). By contrast, we found no change in retina cell number in conditional *Pcdhg*$^{fcon3/tako}$ *trans*-heterozygous retinas (Figures 3A–3E). Like the three C-type genes, the three A-type genes are also expressed in these cell types in the developing retina (Figures S3A and S3B), indicating that the full spectrum of *Pcdhg* isoforms are not required for neuronal survival. Increased levels of apoptosis observed in *Pcdhg*$^{fcon3/tcko}$ *trans*-heterozygous retinas (Figure S3C) are consistent with the previous finding in *Pcdhg*$^{fcon3/fcon3}$ mutants that cell loss and the consequent thinning of IPL is due to elevated programmed cell death (Lefebvre et al., 2008). As with *Pcdhg*$^{fcon3/fcon3}$ mutants, targeting of interneurons and RGC dendrites to appropriate IPL laminae was intact in *Pcdhg*$^{fcon3/tcko}$ *trans*-heterozygous mutants (Figure S3D). Therefore, in the retina as in the spinal cord, removal of the three C-type isoforms results in elevated neuronal apoptosis and loss of specific neuronal subtypes at similar levels and patterns as deletion of all 22 *Pcdhg* isoforms.

Expression and Function of A-Type and B-Type *Pcdhg* Genes Are Not Appreciably Affected in the Absence of C-Type Isoforms

We considered the possibility that the indistinguishable phenotypes of *Pcdhg*$^{tcko/tcko}$ and *Pcdhg*$^{del/del}$ mutants arise because the deletion of C-type exons, which are located immediately upstream of the constant exons, interferes with transcription and splicing of other *Pcdhg* genes, leading to a severely hypomorphic *Pcdhg* allele. To address this possibility, we first examined the expression of the remaining 19 A- and B-type *Pcdhg* genes in *Pcdhg*$^{tcko/tcko}$ brains. RT-PCR using exon-specific primers revealed that all 19 variable exons are expressed and correctly spliced to constant exons (Figures 4A and 4B). Western blotting indicated that Pcdhg total protein levels in *Pcdhg*$^{tcko/tcko}$ brains are similar to the wild-type and even higher than those in *Pcdhg* full cluster deletion

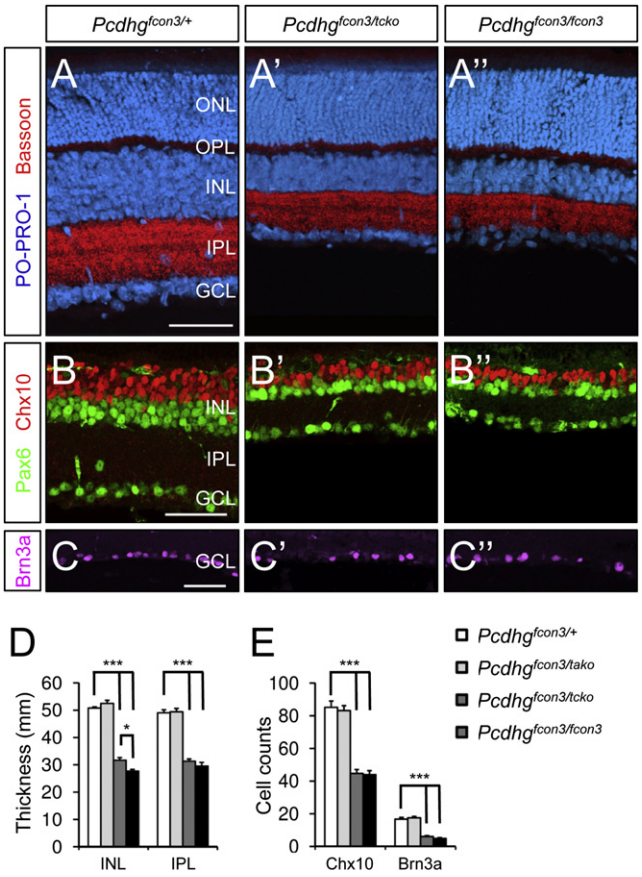

Figure 3. Similar Levels and Patterns of Neuronal Loss in the Retina of *Pcdhg*$^{tcko/tcko}$ and *Pcdhg*$^{del/del}$ Mutants

(A) Nuclear and synaptic layers of retina sections from P18 control and mutants are labeled with Po-Pro1 or anti-Bassoon, respectively. Retinal lamination is normal, and the ONL and OPL thickness are unaffected. INL and IPL thickness are similarly reduced in *Pcdhg*$^{fcon3/tcko}$ and *Pcdhg*$^{fcon3/fcon3}$ mutants but are unaffected in *Pcdhg*$^{fcon3/tako}$ mutants. (B and C) Numbers of Chx10^{+} bipolar (red), Pax6^{+} GABAergic amacrine interneurons (green), as well as Brn3a^{+} projection retinal ganglion cells (magenta) are similarly reduced in *Pcdhg*$^{fcon3/tcko}$ and *Pcdhg*$^{fcon3/fcon3}$ mutants. (D) Quantification of INL and IPL thickness in control and mutant retinas. Error bars represent SEM. *$p < 0.05$, ***$p < 0.01$. (E) Quantification of bipolar interneurons (Chx10) and projection retinal ganglion cells (Brn3a). Error bars represent SEM. ***$p < 0.001$. ONL, outer nuclear layer; OPL, outer plexiform layer; INL, inner nuclear layer; IPL, inner plexiform layer; GCL, ganglion cell layer. Scale bars: 50 μm. See also Figure S3.

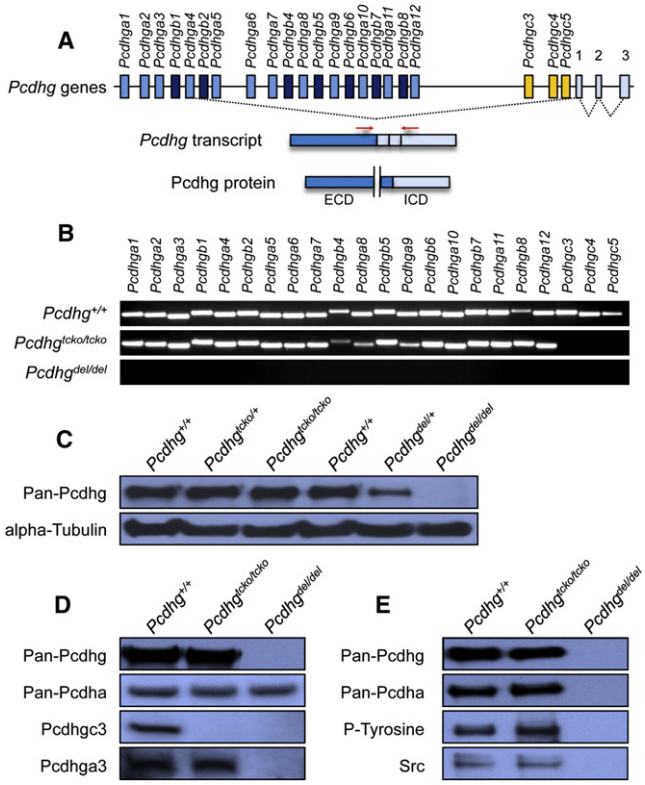

Figure 4. Expression and Function of A- and B-Type Pcdhg Isoforms Are Not Appreciably Affected in the Absence of C-Type Genes

(A) Schematic representation of *Pcdhg* genes, transcripts and proteins. Positions of specific primers (red arrows) are indicated. ECD, extracellular domain; ICD, intracellular domain. (B) RT-PCR of individual *Pcdhg* transcripts in wild-type and both lines of mutants. (C) Western blot indicates that the expression level of Pcdhg proteins in the *Pcdhg*$^{tcko/tcko}$ mutant brain is similar to the wild-type level, but higher than that of *Pcdhg*$^{del/+}$. Alpha tubulin is used as loading control. (D and E) A-type and B-type Pcdhg isoforms in *Pcdhg*$^{tcko/tcko}$ mutant brains still form complexes with Pcdha proteins, remain tyrosine phosphorylated, and mediate signaling. Western blots of P0 brain lysate from wild-type and both mutants are shown in (D), and blots of pan-Pcdhg immunoprecipitates in (E). Transcriptome profiling by RNA-Seq analysis of E13.5 spinal cords found no significant change in globe gene expression in either *Pcdhg*$^{del/del}$ or *Pcdhg*$^{tcko/tcko}$ mutants, but their Pcdh repertoires are differentially altered, as summarized in Figure S4. In addition, no neomorphic *Pcdhg* variants were detected in *Pcdhg*$^{tcko/tcko}$ mutants with splice junction analysis of the RNA-Seq data. Expression levels (RPKMs) of individual exons within the *Pcdh* gene cluster region in wild type and mutant spinal cords are provided in Table S1, and details of the splice junction analysis can be found in Table S2.

heterozygotes, which are phenotypically normal (Figure 4C). We next asked whether the remaining A- and B-type proteins in *Pcdhg*$^{tcko/tcko}$ mutants are functional. Several studies indicate that Pcdhg and Pcdha proteins interact, and may form multimeric complexes with Pcdhb proteins (Han et al., 2010; Murata et al., 2004; Schalm et al., 2010). Moreover, both Pcdha and Pcdhg proteins are tyrosine phosphorylated in mature neurons, suggesting that they mediate intracellular signaling (Schalm et al., 2010). Coimmunoprecipitation experiments using a pan-Pcdhg antibody in brain lysate indicated that the A- and B-type Pcdhg isoforms in *Pcdhg*$^{tcko/tcko}$ mutants still form complexes with Pcdha proteins; they are tyrosine phosphorylated and they interact with Src, suggesting that they are capable of mediating intracellular signaling in the absence of the C-type isoforms (Figures 4D and 4E). We conclude that *Pcdhg*$^{tcko/tcko}$ is not a severe hypomorphic or dominant negative mutant and that expression and function of the remaining A- and B-type Pcdhg isoforms is not appreciably distinct from those of wild-type mice.

To determine whether the expression of a common set of genes is altered in the two phenotypically indistinguishable mutants, we carried out deep sequencing (RNA-Seq) studies

using embryonic spinal cords at E13.5, a developmental stage when neurogenesis is near completion (Nornes and Carry, 1978), but elevated apoptosis is not yet detected in the mutants (Prasad et al., 2008). Surprisingly, we observed no striking changes in global gene expression in either of the two mutants other than those in the *Pcdh* gene clusters themselves (Figures S4A and S4B and Table S1). In the case of $Pcdhg^{del/del}$ mutants, the majority of *Pcdhb* genes are significantly upregulated, likely the consequence of the closer proximity of a *Pcdhb* cluster enhancer (HS16–20) located downstream of the *Pcdhg* cluster (Yokota et al., 2011), which is now repositioned ~300 kb closer to the *Pcdhb* cluster (Figures S4C and S4D). The largest increase in expression is observed with an EST gene (*AK149307*), which is located immediately upstream of the *Pcdhg* cluster (Figures S4C and S4D and Table S1). Sequence analyses revealed that this gene is a relic of the B-type *Pcdhg* isoforms, and its promoter region also contains a conserved sequence element (CSE) found in most *Pcdh* genes (Figures S4E–S4G). The expression levels of most *Pcdhg* isoforms are not affected by the deletion of C-type genes except for a few neighboring ones which are upregulated, and quantification of constant exon reads indicated that the combinatorial expression levels of the remaining *Pcdhg* genes in $Pcdhg^{tcko/tcko}$ mice are ~75% of the wild-type levels (Figures S4C and S4D and Table S1). Thus, the loss of function of the C-type isoforms cannot be compensated by other *Pcdhg* isoforms. Many *Pcdhb* genes (as well as *AK149307*) are marginally upregulated in the $Pcdhg^{tcko/tcko}$ mice, likely also due to the action of the *Pcdhb* cluster enhancer as mentioned above. In addition, no neomorphic *Pcdhg* variants were detected in $Pcdhg^{tcko/tcko}$ mutants with splice junction analysis of the RNA-Seq data (Table S2). The striking phenotypic similarities in contrast to the vastly distinct Pcdh repertoires in $Pcdhg^{tcko/tcko}$ and $Pcdhg^{del/del}$ mutants suggest that lack of the C-type *Pcdhg* isoforms themselves, which is common for both mutants, is the primary cause of the common phenotypes.

Genetically Blocking Apoptosis Rescues the Neonatal Lethality of $Pcdhg^{tcko/tcko}$ Mutants but Not that of $Pcdhg^{del/del}$ Mutants

Since the primary phenotype observed in both $Pcdhg^{tcko/tcko}$ and $Pcdhg^{del/del}$ is neuronal cell death, we crossed both mutant lines to *Bax* knockout mice (Knudson et al., 1995) to compare phenotypes when neuronal apoptosis is genetically blocked. Consistent with previous observations (Weiner et al., 2005), $Pcdhg^{del/del};Bax^{-/-}$ pups show improved neurological function as compared with $Pcdhg^{del/del}$ mutants, yet they still lack voluntary movements, and despite considerable efforts we were unable to recover any $Pcdhg^{del/del};Bax^{-/-}$ mutants beyond P0 (Table 1 and Movie S2). Surprisingly, however, while some $Pcdhg^{tcko/tcko};Bax^{-/-}$ mutants die at P0, many live substantially longer despite being weaker and smaller than wild-type and heterozygous pups. By culling littermates we were able to recover a number of $Pcdhg^{tcko/tcko};Bax^{-/-}$ mutants at weaning age. Some of these animals survived up to 6 months, although their persistent ataxia indicates neurological impairment (Table 1 and Movie S2).

As described for the $Pcdhg^{del/del};Bax^{-/-}$ mutants (Prasad et al., 2008; Weiner et al., 2005), the morphology of spinal cord sections of $Pcdhg^{tcko/tcko};Bax^{-/-}$ is indistinguishable from that of the $Pcdhg^{+/+};Bax^{-/-}$ animals, showing no signs of astrogliosis or microglia activation, and the arborization patterns of IaPA terminals appear largely indistinguishable from those of the controls (Figure S5A). Counts of both $VGAT^+$ and $VGLUT1^+$ inputs onto motor neurons were normal in the $Bax^{-/-}$ genetic background, while $VGLUT2^+$ and $VAChT^+$ synapses remain unchanged (Figure S5B). Therefore, the decreased number of $VGAT^+$ contacts, as well as the increased number of $VGLUT1^+$ contacts and IaPA terminals found in both $Pcdhg^{tcko/tcko}$ and $Pcdhg^{del/del}$ mutants at P0, are both secondary to the cell death of spinal interneurons. These results are reminiscent of findings in the Pcdhg deficient retina in the $Bax^{-/-}$ genetic background, where retinal architecture, cell numbers, and synaptic densities are restored in the absence of neuronal apoptosis (Lefebvre et al., 2008).

Table 1. Genetically Blocking Apoptosis Rescues Neonatal Lethality of $Pcdhg^{tcko/tcko}$ Mutants but Not that of $Pcdhg^{del/del}$ Mutants

Parent Genotypes	Age	# Animals Genotyped	# Single Homozygotes	# Double Homozygotes
$Pcdhg^{tcko/+};Bax^{+/-}$	P0	127	29	16
	P21	191	0	9
$Pcdhg^{del/+};Bax^{+/-}$	P0	89	11	9
	P21	193	0	0

Some normal looking littermates (wild type or heterozygous) were not genotyped and therefore correct genotype ratios cannot be calculated based on these numbers. Single homozygotes: $Pcdhg^{tcko/tcko}$ or $Pcdhg^{del/del}$ mutants that are either $Bax^{+/+}$ or $Bax^{+/-}$; double homozygotes: $Pcdhg^{tcko/tcko};Bax^{-/-}$ or $Pcdhg^{del/del};Bax^{-/-}$ mutants. See also Figure S5 and Movie S2.

DISCUSSION

The Role of the *Pcdhg* Gene Cluster in Neuronal Survival Is Mediated by the C-Type Isoforms

Previous genetic studies using full cluster deletion mutants revealed that Pcdhgs are required for neuronal survival, but the underlying mechanism remains elusive. In this study, we generated mice lacking subsets of *Pcdhg* genes and performed quantitative analyses on specific types of neurons and synapses. Mice lacking C-type *Pcdhg* isoforms are phenotypically indistinguishable from *Pcdhg* null mutants, and the cellular and synaptic changes examined in both the spinal cord and retina are essentially identical. By contrast, mice lacking a subset of A-type isoforms are viable and fertile, revealing at least some level of functional redundancy among the alternative Pcdhg isoforms. Molecular and biochemical analyses demonstrate that deletion of C-type isoforms does not appreciably alter the expression or function of the A-type and B-type isoforms, indicating that the C-type isoform knockouts are not simply hypomorphic or dominant negative for Pcdhg function. Furthermore, transcriptome profiling shows that the Pcdh repertoires of the two mutants differ significantly, but no neomorphic *Pcdhg* variants are generated. Therefore, the loss of function of C-type isoforms themselves is most likely responsible for the identical

phenotypes observed in both the C-type isoform knockouts and the Pcdhg null mutants.

The most remarkable difference between the two types of mutants is that, the neonatal lethality of C-type isoform knockouts can be rescued by genetically blocking apoptosis, while that of the full cluster *Pcdhg* deletion mutants cannot be rescued. The persistence of neonatal lethality in $Pcdhg^{del/del};Bax^{-/-}$ mutants reveals an additional, independent role of Pcdhg isoforms that is required for postnatal development. Therefore, the role of *Pcdhg* cluster in neuronal survival is primarily, if not specifically mediated by the C-type isoforms, whereas the requirement of *Pcdhg* cluster for postnatal development appears to be the collective function of all 22 isoforms in neuronal wiring. Indeed, in a parallel study, we have found dendritic arborization defects in *Pcdhg* null mutants that are not observed in the C-type isoform knockouts (Lefebvre et al., 2012). Hence, similar phenotypes are observed in the $Pcdhg^{tcko/tcko}$ and $Pcdhg^{del/del}$ mutants because the C-type genes are deleted in both lines, and the resulting neuronal cell loss dominates the phenotypes. In the absence of apoptosis, however, the neonatal lethality in C-type isoform knockouts is rescued since neural circuitries essential for postnatal survival are largely preserved by the remaining 19 A-type and B-type Pcdhgs. By contrast, $Pcdhg^{del/del};Bax^{-/-}$ compound mutants still die at P0 since the entire *Pcdhg* cluster is deleted, which severely compromises critical wiring and synaptic function carried out by all isoforms synergistically. The dual role of *Pcdhg* cluster in neuronal survival and neuronal wiring is thus elegantly accomplished by functional and regulatory diversification of its isoforms.

Neuronal Apoptosis Occurs Independently of Synaptic Defects in Pcdhg Deficient Mice

Because of their differential expression, homophilic affinity and synaptic localization, the clustered Pcdhs have been proposed to be the "synaptic adhesive code" that specifies neuronal connectivity (Junghans et al., 2005; Serafini, 1999; Shapiro and Colman, 1999). Therefore, an intuitively attractive hypothesis for the concurrent neuronal apoptosis and synaptic defects in Pcdhg deficient mice is that the loss of function of Pcdhgs leads to synaptic loss, which in turn compromises neuronal survival (Junghans et al., 2005; Prasad et al., 2008). However, several observations reported here strongly argue against this possibility. (1) Deletion of *Pcdhg* cluster does not lead to a general loss of synapses. Instead, we found that *Pcdhg* deficiency differentially influences cholinergic, glutamatergic, GABAergic, and glycinergic synapses on motor neurons. Therefore, the synapse loss observed using generic synaptic markers only reflects the additive effects of alterations in multiple types of synapses, and loss of synaptic contacts, at the very least, cannot explain the loss of neurons in all cases. (2) Consistent with the observations in the retina, the $Pcdhg^{del/del};Bax^{-/-}$ and $Pcdhg^{tcko/tcko};Bax^{-/-}$ compound mutants showed preservation of stretch reflex circuits and major synaptic inputs onto motor neurons, indicating that these severe synaptic defects observed are secondary to interneuron loss. (3) Neural circuitries and synaptic functions are restored to a substantial extent in $Pcdhg^{tcko/tcko};Bax^{-/-}$ mutants, as shown by the rescue of neonatal lethality. If the synaptic defects are primary, they should remain when neuronal apoptosis is blocked by *Bax* deficiency (Buss et al., 2006). This is most likely the case in $Pcdhg^{del/del};Bax^{-/-}$ mutants, which could not be rescued.

Taken together, these observations strongly suggest that neuronal cell death in $Pcdhg^{tcko/tcko}$ and $Pcdhg^{del/del}$ mutants does not result from synaptic defects, but occurs independently due to the lack of C-type genes. Although we cannot rule out the possibility that synaptic or wiring defects may have contributed to the apoptosis of certain types of neurons, it cannot account for the massive cell death observed. In fact, loss of synaptic partners does not usually lead to apoptosis, and even grossly aberrant synaptic connections created experimentally are sometimes maintained without affecting the survival of source neurons (Buss et al., 2006; Oppenheim, 1991).

Functional Similarities and Differences between Vertebrate Pcdhs and Invertebrate Dscams

The vertebrate-specific *Pcdh* gene cluster shares remarkable resemblance with *Drosophila Dscam1* gene in that they both have a complex genomic structure, which encodes a large number of distinct isoforms of cell adhesion molecules with homophilic binding affinity. These parallels have led to the hypothesis that Pcdhs, like Dscams, may provide a source of cell surface diversity for neurite self-recognition and self-avoidance (Zipursky and Sanes, 2010). This possibility is supported by our recent finding of dendritic self-avoidance defects in Pcdhg deficient mice (Lefebvre et al., 2012). A fundamental difference, however, resides in the fact that each Dscam1 isoform appears to be functionally equivalent, whereas certain Pcdhs, such as the C-type isoforms, have unique roles as we show here. Unlike *Dscam1* where isoform diversity is generated by alternative splicing, differential expression of *Pcdh* isoforms is regulated by alternative promoter choice (Tasic et al., 2002; Wang et al., 2002a), which provides precise spatial and temporal controls over gene expression. As noted earlier, the C-type isoforms are phylogenetically unique among Pcdhs and exhibit distinct expression patterns. It remains to be seen whether just one of the three C-type genes is solely responsible for this function, or whether they work synergistically. We note that the two other C-type isoforms in the *Pcdha* cluster (*Pcdhac1* and *Pcdhac2*) are dispensable for neuronal survival (Hasegawa et al., 2008; Katori et al., 2009), but they may play other specific roles yet to be identified. Further functional studies specifically targeting each of these C-type isoforms would be required to address these possibilities.

EXPERIMENTAL PROCEDURES

All animal experimental procedures were in accordance with protocols approved by the Institutional Animal Care and Use Committees (IACUC) of Columbia University Medical Center and Harvard University. Detailed Experimental Procedures can be found in the Supplemental Information with this article online.

SUPPLEMENTAL INFORMATION

Supplemental Information includes five figures, two tables, two movies, and Supplemental Experimental Procedures and can be found with this article online at http://dx.doi.org/10.1016/j.neuron.2012.06.039.

ACKNOWLEDGMENTS

We thank Rick Myers, Rolf Kemler, Greg Philips, Andreas Kolb, and Philippe Soriano for providing essential reagents, Monica Carrasco, Flo Pauli, Jiangwen Zhang, Hilary Bowden, and Amy Kirner for technical assistance, and Tom Jessell, George Mentis, Angel de Blas, Larry Shapiro, and members of the Maniatis laboratory for advice and discussion. This work is funded by NIH grants NS047357 to F.J.A., R01NS029169 to J.R.S., and R01NS043915 to T.M.

Accepted: June 21, 2012
Published: August 8, 2012

REFERENCES

Asada, H., Kawamura, Y., Maruyama, K., Kume, H., Ding, R.G., Kanbara, N., Kuzume, H., Sanbo, M., Yagi, T., and Obata, K. (1997). Cleft palate and decreased brain gamma-aminobutyric acid in mice lacking the 67-kDa isoform of glutamic acid decarboxylase. Proc. Natl. Acad. Sci. USA *94*, 6496–6499.

Buss, R.R., Sun, W., and Oppenheim, R.W. (2006). Adaptive roles of programmed cell death during nervous system development. Annu. Rev. Neurosci. *29*, 1–35.

Chen, H.H., Hippenmeyer, S., Arber, S., and Frank, E. (2003). Development of the monosynaptic stretch reflex circuit. Curr. Opin. Neurobiol. *13*, 96–102.

Esumi, S., Kakazu, N., Taguchi, Y., Hirayama, T., Sasaki, A., Hirabayashi, T., Koide, T., Kitsukawa, T., Hamada, S., and Yagi, T. (2005). Monoallelic yet combinatorial expression of variable exons of the protocadherin-alpha gene cluster in single neurons. Nat. Genet. *37*, 171–176.

Feng, G., Tintrup, H., Kirsch, J., Nichol, M.C., Kuhse, J., Betz, H., and Sanes, J.R. (1998). Dual requirement for gephyrin in glycine receptor clustering and molybdoenzyme activity. Science *282*, 1321–1324.

Fukuda, E., Hamada, S., Hasegawa, S., Katori, S., Sanbo, M., Miyakawa, T., Yamamoto, T., Yamamoto, H., Hirabayashi, T., and Yagi, T. (2008). Down-regulation of protocadherin-alpha A isoforms in mice changes contextual fear conditioning and spatial working memory. Eur. J. Neurosci. *28*, 1362–1376.

Han, M.H., Lin, C., Meng, S., and Wang, X. (2010). Proteomics analysis reveals overlapping functions of clustered protocadherins. Mol. Cell. Proteomics *9*, 71–83.

Hasegawa, S., Hamada, S., Kumode, Y., Esumi, S., Katori, S., Fukuda, E., Uchiyama, Y., Hirabayashi, T., Mombaerts, P., and Yagi, T. (2008). The protocadherin-alpha family is involved in axonal coalescence of olfactory sensory neurons into glomeruli of the olfactory bulb in mouse. Mol. Cell. Neurosci. *38*, 66–79.

Jankowska, E. (1992). Interneuronal relay in spinal pathways from proprioceptors. Prog. Neurobiol. *38*, 335–378.

Junghans, D., Haas, I.G., and Kemler, R. (2005). Mammalian cadherins and protocadherins: about cell death, synapses and processing. Curr. Opin. Cell Biol. *17*, 446–452.

Kaneko, R., Kato, H., Kawamura, Y., Esumi, S., Hirayama, T., Hirabayashi, T., and Yagi, T. (2006). Allelic gene regulation of Pcdh-alpha and Pcdh-gamma clusters involving both monoallelic and biallelic expression in single Purkinje cells. J. Biol. Chem. *281*, 30551–30560.

Katori, S., Hamada, S., Noguchi, Y., Fukuda, E., Yamamoto, T., Yamamoto, H., Hasegawa, S., and Yagi, T. (2009). Protocadherin-alpha family is required for serotonergic projections to appropriately innervate target brain areas. J. Neurosci. *29*, 9137–9147.

Knudson, C.M., Tung, K.S., Tourtellotte, W.G., Brown, G.A., and Korsmeyer, S.J. (1995). Bax-deficient mice with lymphoid hyperplasia and male germ cell death. Science *270*, 96–99.

Kohmura, N., Senzaki, K., Hamada, S., Kai, N., Yasuda, R., Watanabe, M., Ishii, H., Yasuda, M., Mishina, M., and Yagi, T. (1998). Diversity revealed by a novel family of cadherins expressed in neurons at a synaptic complex. Neuron *20*, 1137–1151.

Lefebvre, J.L., Zhang, Y., Meister, M., Wang, X., and Sanes, J.R. (2008). gamma-Protocadherins regulate neuronal survival but are dispensable for circuit formation in retina. Development *135*, 4141–4151.

Lefebvre, J.L., Kostadinov, D., Chen, W.V., Maniatis, T., and Sanes, J.R. (2012). Protocadherins mediate dendritic self-avoidance in the mammalian nervous system. Nature. http://dx.doi.org/10.1038/nature11305, Publsihed online July 29, 2012.

Murata, Y., Hamada, S., Morishita, H., Mutoh, T., and Yagi, T. (2004). Interaction with protocadherin-gamma regulates the cell surface expression of protocadherin-alpha. J. Biol. Chem. *279*, 49508–49516.

Nornes, H.O., and Carry, M. (1978). Neurogenesis in spinal cord of mouse: an autoradiographic analysis. Brain Res. *159*, 1–6.

Oppenheim, R.W. (1991). Cell death during development of the nervous system. Annu. Rev. Neurosci. *14*, 453–501.

Prasad, T., Wang, X., Gray, P.A., and Weiner, J.A. (2008). A differential developmental pattern of spinal interneuron apoptosis during synaptogenesis: insights from genetic analyses of the protocadherin-gamma gene cluster. Development *135*, 4153–4164.

Schalm, S.S., Ballif, B.A., Buchanan, S.M., Phillips, G.R., and Maniatis, T. (2010). Phosphorylation of protocadherin proteins by the receptor tyrosine kinase Ret. Proc. Natl. Acad. Sci. USA *107*, 13894–13899.

Schreiner, D., and Weiner, J.A. (2010). Combinatorial homophilic interaction between gamma-protocadherin multimers greatly expands the molecular diversity of cell adhesion. Proc. Natl. Acad. Sci. USA *107*, 14893–14898.

Serafini, T. (1999). Finding a partner in a crowd: neuronal diversity and synaptogenesis. Cell *98*, 133–136.

Shapiro, L., and Colman, D.R. (1999). The diversity of cadherins and implications for a synaptic adhesive code in the CNS. Neuron *23*, 427–430.

Tasic, B., Nabholz, C.E., Baldwin, K.K., Kim, Y., Rueckert, E.H., Ribich, S.A., Cramer, P., Wu, Q., Axel, R., and Maniatis, T. (2002). Promoter choice determines splice site selection in protocadherin alpha and gamma pre-mRNA splicing. Mol. Cell *10*, 21–33.

Wang, X., Su, H., and Bradley, A. (2002a). Molecular mechanisms governing Pcdh-gamma gene expression: evidence for a multiple promoter and cis-alternative splicing model. Genes Dev. *16*, 1890–1905.

Wang, X., Weiner, J.A., Levi, S., Craig, A.M., Bradley, A., and Sanes, J.R. (2002b). Gamma protocadherins are required for survival of spinal interneurons. Neuron *36*, 843–854.

Weiner, J.A., Wang, X., Tapia, J.C., and Sanes, J.R. (2005). Gamma protocadherins are required for synaptic development in the spinal cord. Proc. Natl. Acad. Sci. USA *102*, 8–14.

Wojcik, S.M., Katsurabayashi, S., Guillemin, I., Friauf, E., Rosenmund, C., Brose, N., and Rhee, J.S. (2006). A shared vesicular carrier allows synaptic corelease of GABA and glycine. Neuron *50*, 575–587.

Wu, Q., and Maniatis, T. (1999). A striking organization of a large family of human neural cadherin-like cell adhesion genes. Cell *97*, 779–790.

Wu, Q., Zhang, T., Cheng, J.F., Kim, Y., Grimwood, J., Schmutz, J., Dickson, M., Noonan, J.P., Zhang, M.Q., Myers, R.M., and Maniatis, T. (2001). Comparative DNA sequence analysis of mouse and human protocadherin gene clusters. Genome Res. *11*, 389–404.

Yokota, S., Hirayama, T., Hirano, K., Kaneko, R., Toyoda, S., Kawamura, Y., Hirabayashi, M., Hirabayashi, T., and Yagi, T. (2011). Identification of the cluster control region for the protocadherin-beta genes located beyond the protocadherin-gamma cluster. J. Biol. Chem. *286*, 31885–31895.

Zipursky, S.L., and Sanes, J.R. (2010). Chemoaffinity revisited: dscams, protocadherins, and neural circuit assembly. Cell *143*, 343–353.